THE JOURNAL OF PHYSICAL CHEMISTRY Letters

Letter

pubs.acs.org/JPCL

Time-Resolved Photodetachment Anisotropy: Gas-Phase Rotational and Vibrational Dynamics of the Fluorescein Anion

Daniel A. Horke,[†] Adam S. Chatterley,[‡] James N. Bull,[§] and Jan R. R. Verlet*[,§]

[†]Center for Free-Electron Laser Science, DESY, Notkestrasse 85, 22607 Hamburg, Germany

[‡]Ultrafast X-ray Science Laboratory, Cyclotron Road, Berkeley, California 94720, United States

[§]Department of Chemistry, University of Durham, South Road, Durham DH1 3LE, United Kingdom

Supporting Information

ABSTRACT: The photoelectron signal of the singly deprotonated fluorescein anion is found to be highly dependent on the relative polarization between pump and probe pulses, and time-resolved photodetachment anisotropy (TR-PA) is developed as a probe of the rotational dynamics of the chromophore. The total photoelectron signal shows both rotational and vibrational wavepacket dynamics, and we demonstrate how TR-PA can readily disentangle these dynamical processes. TR-PA in fluorescein presents specific opportunities for its development as a probe for rotational dynamics in large biomolecules as fluorescein derivatives are commonly incorporated in complex biomolecules and have been used extensively in time-resolved fluorescence anisotropy measurements, to which TR-PA is a gas-phase analogue.

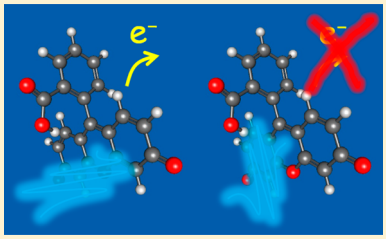

The measurement and control over molecular alignment has been an important tool in both solution and gas-phase chemical physics and biophysics, as it provides a route to monitoring structural change and controlling molecular dynamics. For example, time-resolved fluorescence anisotropy (TR-FA) and imaging have enabled the direct probing of biophysical processes,[1−3] while alignment experiments in the gas phase have opened up countless avenues for probing molecular-frame processes.[4−6] Some of the experimental tools are transferable between solution and gas phases, and fluorescence measurements have elegantly demonstrated their potential power in large isolated molecular systems,[7−14] including distance measurements using Förster resonance energy transfer (FRET).[14−20] TR-FA, in particular, has been very informative in biophysics, and, consequently, it also has great potential to become an important analytical tool in structure and function determination in the gas phase; however, this premise has yet to be fully realized. This is in part due to technical difficulties such as the low density of ions stored in typical ions traps and the limited photon collection efficiencies that ultimately render time-resolved fluorescence experiments rather difficult. We describe an approach to monitoring rotational dynamics based on time-resolved photodetachment anisotropy (TR-PA) and demonstrate the methodology on the fluorescein anion, which is an important marker in fluorescence imaging. From a chemical physics perspective, we show that TR-PA can readily disentangle rotational from vibrational and population dynamics, which is pertinent to many time-resolved gas-phase experiments such as time-resolved photoelectron spectroscopy.[21−23] The demonstration of TR-PA on fluorescein holds significant potential as a probe for the dynamics of much large biomolecular assemblies and as a use in, for example, gas-phase FRET.

TR-PA, similar to its fluorescence analogue, relies on a polarized light pulse to create a coherent rotational superposition upon excitation of a bright transition in a chromophore. As the transition dipole moment for the excitation is aligned along a given molecular axis, only a subpopulation of the randomly oriented ensemble will be excited. Specifically, molecules distributed as a $\cos^2\theta$ distribution, where θ is the angle between the polarization and transition dipole moment, will be excited. In fluorescence anisotropy measurements, one then requires fluorescence and, if this occurs via the same transition as excitation, then photons emitted immediately after excitation will be polarized along the same axis as the excitation light. As a function of time, the polarization of the fluorescence will become isotropic as the molecule undergoes rotational dynamics. Hence, by monitoring the polarization of the fluorescence as a function of time, information about the rotational dephasing time can be obtained, which, in turn, is dependent on the rotational constants of the system. The limitations of this method are that (i) it requires a fluorophore; (ii) the efficiency of photon detection is limited by the limited solid angle of fluorescence collected and the detector efficiency (typically a photomultiplier tube); and (iii) the time resolution is limited by the data acquisition hardware (typically in the picosecond range).

In TR-PA, the excitation step is the same as in TR-FA. As a probe, however, photodetachment is performed from the excited state in a traditional pump−probe fashion. The anisotropy in this case stems from an anisotropy in the

Received: October 24, 2014
Accepted: December 21, 2014
Published: December 22, 2014

DOI: 10.1021/jz5022526
J. Phys. Chem. Lett. 2015, 6, 189−194

differential photodetachment cross section from the excited state. If this is strongly aligned along a specific molecular axis (be it parallel or perpendicular to the transition dipole moment for initial excitation), then the cross section for electron emission will exhibit a strong dependence on the polarization of the probe. Hence, a measurement of the *total* photoelectron yield as a function of time for a probe polarized parallel and perpendicular to the initial excitation field will yield similar information as TR-FA.

Here we demonstrate TR-PA on the fluorescein anion, $[fl\text{-}H]^-$, which is predominantly deprotonated on the xanthene moiety in the gas phase and at the benzoic acid in solution.[24] Fluorescein is a typical and widely used biomarker[3] because it can be functionalized (for example, fluorescein-isothiocyanate (FITC)) for attaching to biological species of interest. $[fl\text{-}H]^-$ has been extensively studied in solution and to a lesser extent in the gas phase. The anion has an electron affinity of ~3.5 eV. The $S_1 \leftarrow S_0$ transition measured by action spectroscopy is a broad feature that has a maximum at 2.4 eV (525 nm) (which is red-shifted relative to solution).[25] In the gas phase, the $[fl\text{-}H]^-$ has a low fluorescence quantum yield.[26] Despite this, the lifetime of the excited states of monoanionic fluorescein derivatives has been determined to be ~5 ns in the gas phase.[26] For the TR-PA experiments described here, the bright $S_1 \leftarrow S_0$ transition was excited at 2.51 eV (495 nm), launching a rovibrational wavepacket on the S_1 excited state. This was subsequently probed at a variable delay later through photodetachment with a 3.10 eV (400 nm) pulse. This scheme is summarized in Figure 1. The $S_1 \leftarrow S_0$ transition dipole moment is well-defined and aligned along the xanthene moiety of $[fl\text{-}H]^-$. (See Figure 1.) As we show later, the photodetachment from the S_1 state is also highly directional and, combined with the long lifetime of the excited state, makes $[fl\text{-}H]^-$ a well-suited system to demonstrate and apply TR-PA.

Experiments were conducted using a femtosecond photoelectron imaging spectrometer coupled to an electrospray ionization source.[27,28] Briefly, $[fl\text{-}H]^-$ was generated by electrospray ionization of a 1 mM solution of fluorescein in methanol at −2.5 kV. Anions were trapped in a ring-electrode trap, where they thermalize to ~300 K, and were injected at 500 Hz into a Wiley−McLaren time-of-flight spectrometer. Under the conditions used in the current experiment, ejection from the trap can lead to a moderate heating of the ions, and the temperature can be roughly controlled by changing the ejection potentials from the trap. The mass-selected $[fl\text{-}H]^-$ ion packet was intersected perpendicularly by femtosecond pump and probe pulses at the center of a velocity-map imaging spectrometer.[29] The photoelectron spectrometer was used only to monitor the total electron yield by counting the total signal observed on the position sensitive detector using a charge-coupled device camera. Femtosecond pump and probe laser pulses were derived from a commercial Ti:sapphire oscillator and amplifier system, delivering 35 fs pulses at a 500 Hz repetition rate. Pump pulses in the visible were generated by mixing the signal output at 0.96 eV (1300 nm) from an optical parametric amplifier with remaining fundamental 1.55 eV (800 nm) light. Probe pulses at 3.10 eV (400 nm) were obtained from frequency doubling in a beta-barium borate (BBO) crystal. The delay between pump and probe pulses was controlled via an optical delay line. The pump−probe cross correlation was measured in an additional BBO crystal as ~130 fs, and the full width at half-maximum bandwidth of both pump and probe pulses was ~30 meV. Pulses enter the interaction region unfocused but collimated to ~2 mm diameter, yielding intensities on the order of 3×10^{10} W cm^{-2}. The relative polarization of pump and probe pulses was controlled with a $\pi/2$ waveplate in the probe path; the pump was always polarized parallel to the detector face.

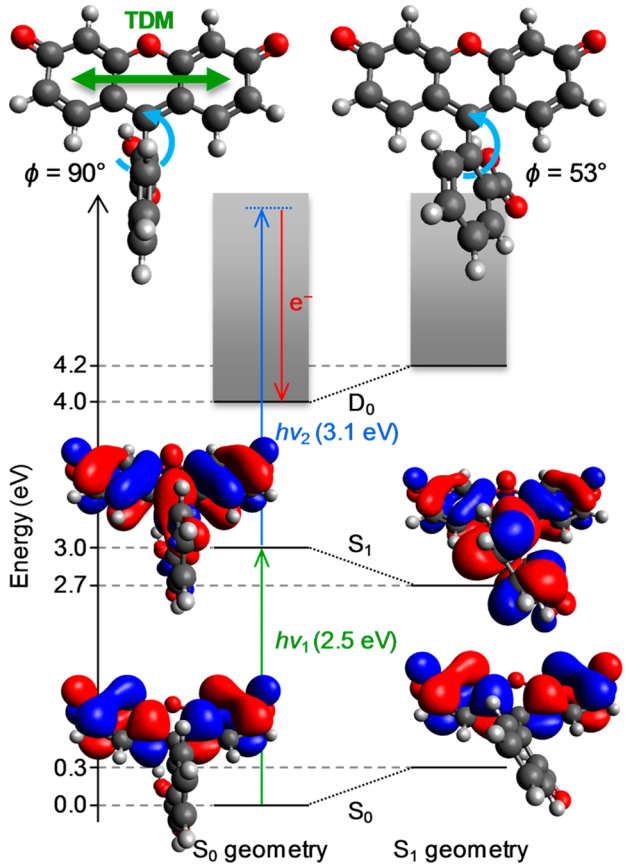

Figure 1. Excitation scheme of the deprotonated fluorescein anion along with calculated energies and the relevant molecular orbitals. Photon energies used in experiment are also indicated. The main structural rearrangement between the S_0 and S_1 state minimum energy geometries is a rotation about the dihedral angle ϕ, as shown at the top, along with the transition dipole moment (TDM) vector for the $S_1 \leftarrow S_0$ transition.

To support interpretations of the data, we have also performed density functional theory (DFT) and time-dependent (TD-) DFT calculations, which were performed at the 6-31++G(d,p) level using the ωB97XD and CAM-B3LYP functionals within the Gaussian 09 software package.[30−33] Briefly, these two functionals incorporate long-range dispersion and nonlocal Hartree−Fock exchange corrections, which are known to be important for the correct description of molecular anions and for excited states involving significant charge-transfer character.[34,35] Optimized geometries were confirmed to be the minimum energy structures through harmonic vibrational frequency analysis. The CAM-B3LYP functional consistently produced energetics within 0.2 eV of those using the ωB97XD functional. Note, however, that the level of theory was not chosen to achieve quantitative agreement with experiment but instead as an aide to a qualitative interpretation of the dynamics. The parameter ϕ is the dihedral angle between the planes defining the xanthene and benzoic acid rings, as shown in Figure 1.

DOI: 10.1021/jz5022526
J. Phys. Chem. Lett. 2015, 6, 189−194

The photoelectron yield as a function of pump−probe delay is shown in Figure 2 for parallel (red) and perpendicular (blue) relative polarizations of the pump and probe beams. Both traces have been normalized to unity at long delay times. The parallel component shows a very fast rise at $t = 0$, with a rise time corresponding to the instrument response function of ∼130 fs, followed by an exponential decay on a picosecond time scale. Additionally, the total photoelectron yield is strongly modulated by an oscillatory component with a period of ∼1 ps. Both the decay and oscillation disappear after a few picoseconds, and the signal remains constant from thereon over the temporal window probed (100 ps). When the probe is perpendicular to the pump, the signal rises near $t = 0$ but does not reach the level seen for parallel pump−probe polarizations and then gradually increases on a picosecond time scale to the level for parallel polarizations at long delays. Superimposed on this is a modulation of the photoelectron yield, of similar period to that observed for parallel polarizations and with the same phase.

Both the parallel and perpendicular polarization TR-PA could be modeled using a simple exponential decay and rise, respectively, modulated by a damped cosine oscillation and convoluted with the 130 fs instrument response function. The resulting fits are shown as solid lines in Figure 2 and have a common exponential lifetime and oscillation frequency, phase, and amplitude. The exponential lifetime is found to be $\tau_r = 725 \pm 70$ fs, while the oscillation period is $\tau_v = 1050 \pm 100$ fs.

Although exponential decays measured in a total photoelectron yield experiment can often be correlated with electronic dynamics,[21−23,36] in the present case this is clearly invalid as such dynamics should not normally depend on the relative polarization of the pump and probe. Instead, it appears that the observed dynamics are dominated by the anisotropy of the photodetachment process. This can be clearly demonstrated by employing an analysis methodology analogous to that used in TR-FA. Namely, we define the photoelectron emission anisotropy, $r(t)$, as the difference between the photoelectron signal following parallel $I_{//}$ and perpendicular $I_\perp$ probe pulses, relative to the total signal $I = I_{//} + 2I_\perp$

$$r(t) = \frac{I_{//} - I_\perp}{I_{//} + 2I_\perp}$$

The anisotropy function $r(t)$ based on our data is shown in Figure 3a. This has recovered only the decay component and is a sensitive measure of the rotational dephasing dynamics. It is common in TR-FA to model $r(t)$ as an exponential decay: $r(t) = r_0 \exp(-t/\tau_r)$, where $\tau_r = 725$ fs is the rotational correlation time and r_0 is the initial anisotropy, which ranges from 0.4 to −0.2. In TR-PA, this corresponds to a differential photodetachment cross section peaking parallel to or perpendicular to the excitation transition dipole moment, respectively. From Figure 3a, $r_0 = 0.34$, indicating that the differential photodetachment cross section is strongly peaking along the xanthene unit.

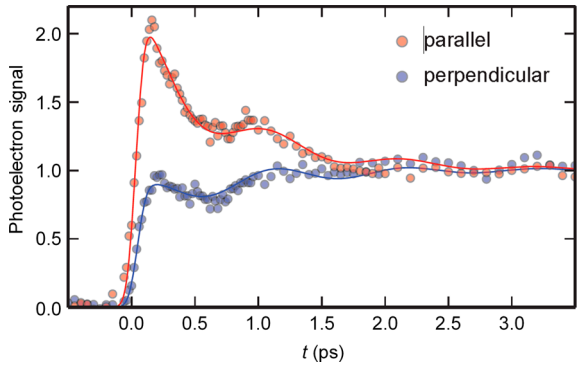

Figure 2. Total photoelectron signal monitored as a function of time delay between pump and probe when their relative pump−probe polarization is parallel and perpendicular.

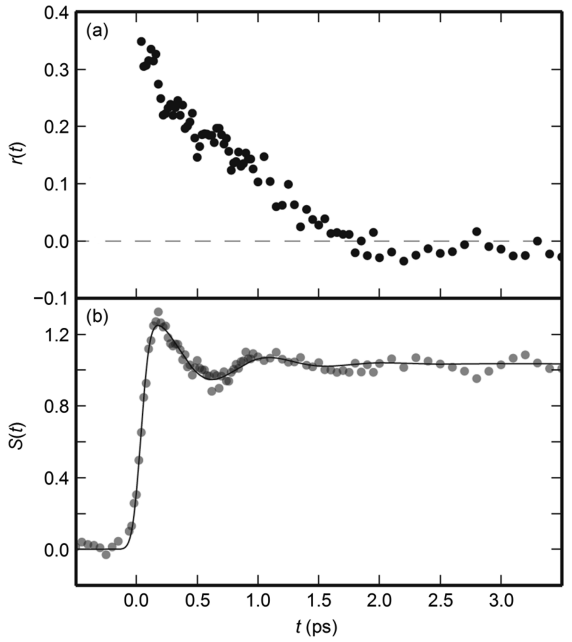

Figure 3. (a) Time-resolved photoelectron anisotropy, $r(t)$, showing the rotational dephasing of fluorescein and (b) time-resolved isotropic signal function, $S(t)$, showing the population dynamics on the S_1 state as well as vibrational wavepacket dynamics.

The rotational dynamics observed originate from the evolution of a rotational coherence formed upon excitation to the S_1 excited state, as discussed in detail by Felker and Zewail.[10,11] The fast decay of the rotational coherence is due to the dephasing of the rotational wavepacket,[37] and after ∼2 ps, the average laboratory-frame alignment in the excited state is lost. This dephasing depends on the rotational constants and the initial temperature. The minimum in the anisotropy function can be estimated for an asymmetric rotor (with moments of inertia, $I_x > I_y > I_z$) using $t_{min} \approx (I_y/k_BT)^{1/2}$.[37] Using $I_y = 3.670 \times 10^{-44}$ kg m^2 and $t_{min} \approx 2.2$ ps (from Figure 3a), an internal temperature of $T \approx 550$ K is obtained. We have also performed our experiments under "colder" conditions, which revealed that the rotational dephasing indeed slows down to $t_{min} \approx 3$ ps, corresponding to an internal temperature of $T \sim 300$ K. (See the Supporting Information.)[38,39] A full analysis of the rotational dephasing would allow an accurate determination of the rotational constants of a molecular system from τ_r;[37] however, as this requires an accurate determination of the internal temperature, such an analysis is beyond the scope of this study. In TR-FA, τ_r can be related to the local viscosity of the solvent, which is clearly not appropriate for a gas-phase experiment. However, comparison of TR-FA of a molecule in solution with TR-PA in the gas phase would provide an interesting comparison. Unfortunately, such a direct comparison is again sensitively dependent on temperature in the gas phase, which we currently cannot accurately control.

DOI: 10.1021/jz5022526
J. Phys. Chem. Lett. 2015, 6, 189−194

Experiments are currently underway in our laboratory in which the temperature can be controlled.

Revivals and fractional revivals in the rotational wavepacket should also be observable; full revivals for a diatomic occur at $(2Bc)^{-1}$, where B (m^{-1}) is the rotational constant.[4] For an asymmetric rotor (fluorescein), the three rotational constants significantly complicate the revival pattern. We have not observed such revivals in the present study and point out that these would occur on time scales well beyond that probed in the present experiments. We note that for the discussion of incorporation of fluorescein as a marker in a larger molecular system, such rotational revivals would occur on even longer time scales (many nanoseconds) and will additionally be blurred by thermal fluctuations in the structure. Hence, these would be very difficult to observe experimentally.

A striking feature of $r(t)$ in Figure 3a is that the oscillations are completely removed, which indicates that these modulations seen in Figure 2 do not depend on the relative polarization of the pulses. Oscillations on top of a photoelectron signal are indicative of vibrational wavepacket motion.[21,22,40] In a similar manner to the analysis yielding the anisotropy parameter, we can again borrow tools from TR-FA. The isotropic signal function, $S(t)$, can be defined as

$$S(t) = \frac{1}{3}(I_{//} + 2I_{\perp})$$

and the results for $S(t)$ applied to our data are shown in Figure 3b. It clearly recovers the vibrational dynamics (in this case a quantum beat) present in the data as well as the population dynamics, which simply involve the step function with width defined by the cross correlation (i.e., excitation of $S_1 \leftarrow S_0$). The oscillations are strongly damped and disappear within the first few picoseconds.

Given the size of the molecular system and the rigidity of the xanthene unit, the period of the vibrational wavepacket is remarkably slow, τ_v = 1050 fs, corresponding to a vibrational wavenumber of 32 cm^{-1}. To gain a qualitative insight into the possible dynamics that are observed in the experiment, we turn to results from our calculations, which are summarized in Figure 1 (calculated energies are given in the Supporting Information). In the ground S_0 state, the two ring systems are perpendicular to each other and the dihedral angle between the xanthene and benzoic acid groups ϕ = 90°. The $S_1 \leftarrow S_0$ photoexcitation involves a $\pi^*_{LUMO} \leftarrow \pi_{HOMO}$ transition, in which both orbitals are localized predominantly on the xanthene group. Initially, the π^*_{LUMO} does not interact with any π^* orbitals on the benzoic acid group due to incompatible symmetry at ϕ = 90°. The principal motion in geometrical relaxation of the S_1 state involves rotation of the benzoic acid with respect to the xanthene, reaching a minimum energy geometry with ϕ = 53°. This torsional motion is accompanied by a partial charge transfer from the π^*_{LUMO} on the xanthene group, which can now mix with π^* orbitals on the benzoic acid group. Although there is also a small twisting distortion of the xanthene and a bend of the benzoic acid out of the plane of the xanthene unit, the torsional mode about ϕ is by far the most prominent. We have calculated the frequencies of vibrational modes of the S_1 excited state, and these show that there are six modes with frequencies less than 100 cm^{-1}. The lowest energy vibrational mode corresponds to the ϕ torsion, which has a calculated wavenumber of 35.6 cm^{-1}. This corresponds to a period of 940 fs, which is in excellent agreement with the observed wavepacket motion in Figure 3b. The observation of the torsional motion in the total photoelectron yield may be explained by either the fact that the Franck−Condon window for detachment from the S_1 has become smaller by ∼0.4 eV (see Figure 1) or the cross-section for detachment changes along the torsional coordinate. The latter might be expected given that the electronic character is changing quite substantially. However, if this were the case, then one might also anticipate that the differential cross sections might change, which would be reflected in $r(t)$, which it is not. The charge-transfer nature of the S_1 excited state has been controversially discussed in the literature,[41−43] and our indications suggest that a partial electron transfer does occur, at least in the gas phase.

The ability to measure and decouple the rotational dynamics from population and vibrational dynamics in the time-resolved photoelectron yield is very useful. Indeed, the interpretation of time-resolved photoelectron spectroscopic data can sensitively depend on such dynamics, and rotational dynamics have been misinterpreted as population dynamics.[44,45] Simply measuring the total ion yield with two polarizations would eliminate such ambiguities. In cases where population dynamics are occurring on very different time scales as rotational dephasing, as is the case for nucleotides and oligonucleotides,[46,47] for example, such complications are less important. Extending the measurement to arbitrary angles between the two polarizations (i.e., between the alignment axis and the detachment polarization) near t = 0 allows the direct measurement of the angle between the aligned axis of the molecule and the preferential direction for electron detachment (differential cross-section). TR-PA is therefore also a viable methodology to quantitatively measure the degree of molecular alignment without relying on fragment imaging of the target molecule. This is especially applicable when extending existing alignment methods to larger systems where fragmentation often produces many same-mass fragments or when the kinetic energy released exhibits considerable energy spread.

The fact that r_0 = 0.34 is close to its maximum value of 0.4 in the present case suggests that fluorescein may present an outstanding probe to monitoring rotational dynamics in larger systems. If tightly bound within a large protein complex that inhibits fluorescein rotation, the dynamics probed through TR-PA would correspond to the rotational motion of the protein complex and one can extract rotational constants from the complex. Consequently, one can infer structural information about the complex and TR-PA would provide complementary information to ion mobility spectrometry.[48,49] Alternatively, it would also provide a sensitive probe of the "friction" of a large biomolecule in solution, as it can now be directly compared with a frictionless (i.e., gas-phase) environment. Moreover, applications using FRET can be envisaged using fluorescein that can provide information about intramolecular distances and dynamics.

Although closely related to TR-FA, TR-PA has some distinct advantages when applied to gas-phase ions. The photodetached electron can be detected with near unit efficiency, in contrast with fluorescence, in which the collection optics lead to significant losses, as does the ultimate detection, which is often based on photomultiplier technology. Admittedly, an additional photon is required to photodetach from the excited state in TR-PA, but the efficient means by which the photoelectron can be detected makes this acceptable. The temporal resolution in TR-PA is determined by a pump−probe scheme and is therefore limited to the duration of the laser pulses (tens of femtoseconds), in contrast with single-pulse fluorescence measure-

DOI: 10.1021/jz5022526
J. Phys. Chem. Lett. 2015, 6, 189−194

ments that are limited by data acquisition hardware of time-correlated single photon counting systems (tens of picoseconds). In solution-phase fluorescence experiments, ultrafast time resolution is accessible by using fluorescence up-conversion, but this has not been demonstrated in the gas phase due to the prohibitively low ion densities. Finally, in principle, no fluorophore is required, and only a chromophore is needed as long as its excited-state lifetime is sufficiently long to observe rotational dynamics and the excited-state photoemission shows a strongly anisotropic differential cross section.

In summary, we have demonstrated TR-PA as a useful method for probing rotational dynamics. Specifically, we have demonstrated this here for the fluorescein anion, which holds particular promise as a label in larger gas-phase biomolecules in which the method could be developed as a sensitive probe of structure and dynamics. The rotational dynamics for fluorescein indicate that it has very strong inherent photodetachment anisotropy from the S_1 state.

■ ASSOCIATED CONTENT

Supporting Information

Temperature dependence of rotational dephasing and details of calculations. This material is available free of charge via the Internet at http://pubs.acs.org.

■ AUTHOR INFORMATION

Corresponding Author

*E-mail: j.r.r.verlet@durham.ac.uk.

Notes

The authors declare no competing financial interest.

■ ACKNOWLEDGMENTS

This work was funded by the Leverhulme Trust, the ERC (306536), and the EPSRC.

■ REFERENCES

(1) Royer, C. A. Probing Protein Folding and Conformational Transitions with Fluorescence. *Chem. Rev.* **2006**, *106*, 1769−1784.

(2) Rao, J.; Dragulescu-Andrasi, A.; Yao, H.; Yao, H. Fluorescence Imaging in Vivo: Recent Advances. *Curr. Opin. Biotechnol.* **2007**, *18*, 17−25.

(3) Jameson, D. M.; Ross, J. A. Fluorescence Polarization/Anisotropy in Diagnostics and Imaging. *Chem. Rev.* **2010**, *110*, 2685−2708.

(4) Stapelfeldt, H.; Seideman, T. Colloquium: Aligning Molecules with Strong Laser Pulses. *Rev. Mod. Phys.* **2003**, *75*, 543−557.

(5) Bisgaard, C. Z.; Clarkin, O. J.; Wu, G. R.; Lee, A. M. D.; Gessner, O.; Hayden, C. C.; Stolow, A. Time-Resolved Molecular Frame Dynamics of Fixed-in-Space Cs2Molecules. *Science* **2009**, *323*, 1464−1468.

(6) Brouard, M.; Parker, D. H.; van de Meerakker, S. Y. T. Taming Molecular Collisions Using Electric and Magnetic Fields. *Chem. Soc. Rev.* **2014**, *43*, 7279−7294.

(7) Nagy, A. M.; Talbot, F. O.; Czar, M. F.; Jockusch, R. A. Fluorescence Lifetimes of Rhodamine Dyes in Vacuo. *J. Photochem. Photobiol., A* **2012**, *244*, 47−53.

(8) Iavarone, A. T.; Parks, J. H. Conformational Change in Unsolvated Trp-Cage Protein Probed by Fluorescence. *J. Am. Chem. Soc.* **2005**, *127*, 8606−8607.

(9) Nathanson, G. M.; McClelland, G. M. Fluorescence Polarization as a Probe of the Rotational-Dynamics of Isolated Highly Excited Molecules. *J. Chem. Phys.* **1984**, *81*, 629−642.

(10) Felker, P. M.; Baskin, J. S.; Zewail, A. H. Rephasing of Collisionless Molecular Rotational Coherence in Large Molecules. *J. Phys. Chem.* **1986**, *90*, 724−728.

(11) Felker, P. M.; Zewail, A. H. Purely Rotational Coherence Effect and Time-Resolved Sub-Doppler Spectroscopy of Large Molecules 0.1. Theoretical. *J. Chem. Phys.* **1987**, *86*, 2460−2482.

(12) Khoury, J. T.; Rodriguez-Cruz, S. E.; Parks, J. H. Pulsed Fluorescence Measurements of Trapped Molecular Ions with Zero Background Detection. *J. Am. Soc. Mass. Spectrom.* **2002**, *13*, 696−708.

(13) Shi, X.; Parks, J. H. Fluorescence Lifetime Probe of Biomolecular Conformations. *J. Am. Soc. Mass. Spectrom.* **2010**, *21*, 707−718.

(14) Iavarone, A. T.; Duft, D.; Parks, J. H. Shedding Light on Biomolecule Conformational Dynamics Using Fluorescence Measurements of Trapped Ions. *J. Phys. Chem. A* **2006**, *110*, 12714−12727.

(15) Danell, A. S.; Parks, J. H. Fret Measurements of Trapped Oligonucleotide Duplexes. *Int. J. Mass Spectrom.* **2003**, *229*, 35−45.

(16) Dashtiev, M.; Azov, V.; Frankevich, V.; Scharfenberg, L.; Zenobi, R. Clear Evidence of Fluorescence Resonance Energy Transfer in Gas-Phase Ions. *J. Am. Soc. Mass. Spectrom.* **2005**, *16*, 1481−1487.

(17) Iavarone, A. T.; Patriksson, A.; van der Spoel, D.; Parks, J. H. Fluorescence Probe of Trp-Cage Protein Conformation in Solution and in Gas Phase. *J. Am. Chem. Soc.* **2007**, *129*, 6726−6735.

(18) Talbot, F. O.; Rullo, A.; Yao, H.; Jockusch, R. A. Fluorescence Resonance Energy Transfer in Gaseous, Mass-Selected Polyproline Peptides. *J. Am. Chem. Soc.* **2010**, *132*, 16156−16164.

(19) Daly, S.; Poussigue, F.; Simon, A.-L.; MacAleese, L.; Bertorelle, F.; Chirot, F.; Antoine, R.; Dugourd, P. Action-Fret: Probing the Molecular Conformation of Mass-Selected Gas-Phase Peptides with Forster Resonance Energy Transfer Detected by Acceptor-Specific Fragmentation. *Anal. Chem.* **2014**, *86*, 8798−8804.

(20) Frankevich, V.; Chagovets, V.; Widjaja, F.; Barylyuk, K.; Yang, Z.; Zenobi, R. Fluorescence Resonance Energy Transfer of Gas-Phase Ions under Ultra High Vacuum and Ambient Conditions. *Phys. Chem. Chem. Phys.* **2014**, *16*, 8911−8920.

(21) Stolow, A.; Bragg, A. E.; Neumark, D. M. Femtosecond Time-Resolved Photoelectron Spectroscopy. *Chem. Rev.* **2004**, *104*, 1719−1757.

(22) Suzuki, T. Femtosecond Time-Resolved Photoelectron Imaging. *Annu. Rev. Phys. Chem.* **2006**, *57*, 555−592.

(23) Verlet, J. R. R. Femtosecond Spectroscopy of Cluster Anions: Insights into Condensed-Phase Phenomena from the Gas-Phase. *Chem. Soc. Rev.* **2008**, *37*, 505−517.

(24) Yao, H.; Steill, J. D.; Oomens, J.; Jockusch, R. A. Infrared Multiple Photon Dissociation Action Spectroscopy and Computational Studies of Mass-Selected Gas-Phase Fluorescein and 2 ′,7 ′-Dichlorofluorescein Ions. *J. Phys. Chem. A* **2011**, *115*, 9739−9747.

(25) McQueen, P. D.; Sagoo, S.; Yao, H.; Jockusch, R. A. On the Intrinsic Photophysics of Fluorescein. *Angew. Chem., Int. Ed.* **2010**, *49*, 9193−9196.

(26) Yao, H.; Jockusch, R. A. Fluorescence and Electronic Action Spectroscopy of Mass-Selected Gas-Phase Fluorescein, 2 ′,7 ′-Dichlorofluorescein, and 2 ′,7 ′-Difluorofluorescein Ions. *J. Phys. Chem. A* **2013**, *117*, 1351−1359.

(27) Lecointre, J.; Roberts, G. M.; Horke, D. A.; Verlet, J. R. R. Ultrafast Relaxation Dynamics Observed through Time-Resolved Photoelectron Angular Distributions. *J. Phys. Chem. A* **2010**, *114*, 11216−11224.

(28) Horke, D. A.; Verlet, J. R. R. Time-Resolved Photoelectron Imaging of the Chloranil Radical Anion: Ultrafast Relaxation of Electronically Excited Electron Acceptor States. *Phys. Chem. Chem. Phys.* **2011**, *13*, 19546−19552.

(29) Horke, D. A.; Roberts, G. M.; Lecointre, J.; Verlet, J. R. R. Velocity-Map Imaging at Low Extraction Fields. *Rev. Sci. Instrum.* **2012**, 83.

(30) Chai, J.-D.; Head-Gordon, M. Long-Range Corrected Hybrid Density Functionals with Damped Atom-Atom Dispersion Corrections. *Phys. Chem. Chem. Phys.* **2008**, *10*, 6615−6620.

(31) Frisch, M. J.; Trucks, G. W.; Schlegel, H. B.; Scuseria, G. E.; Robb, M. A.; Cheeseman, J. R.; Scalmani, G.; Barone, V.; Mennucci, B.; Petersson, G. A.; Nakatsuji, H.; Caricato, M.; Li, X.; Hratchian, H. P.; Izmaylov, A. F.; Bloino, J.; Zheng, G.; Sonnenberg, J. L.; Hada, M.;

DOI: 10.1021/jz5022526
J. Phys. Chem. Lett. 2015, 6, 189−194

Ehara, M.; Toyota, K.; Fukuda, R.; Hasegawa, J.; Ishida, M.; Nakajima, T.; Honda, Y.; Kitao, O.; Nakai, H.; Vreven, T.; Montgomery, J. A., Jr.; Peralta, J. E.; Ogliaro, F.; Bearpark, M.; Heyd, J. J.; Brothers, E.; Kudin, K. N.; Staroverov, V. N.; Kobayashi, R.; Normand, J.; Raghavachari, K.; Rendell, A.; Burant, J. C.; Iyengar, S. S.; Tomasi, J.; Cossi, M.; Rega, N.; Millam, M. J.; Klene, M.; Knox, J. E.; Cross, J. B.; Bakken, V.; Adamo, C.; Jaramillo, J.; Gomperts, R.; Stratmann, R. E.; Yazyev, O.; Austin, A. J.; Cammi, R.; Pomelli, C.; Ochterski, J. W.; Martin, R. L.; Morokuma, K.; Zakrzewski, V. G.; Voth, G. A.; Salvador, P.; Dannenberg, J. J.; Dapprich, S.; Daniels, A. D.; Farkas, Ö.; Foresman, J. B.; Ortiz, J. V.; Cioslowski, J.; Fox, D. J. *Gaussian 09*, revision A.01; Gaussian, Inc.: Wallingford, CT, 2009.

(32) Hehre, W. J.; Ditchfie, R.; Pople, J. A. Self-Consistent Molecular-Orbital Methods 0.12. Further Extensions of Gaussian-Type Basis Sets for Use in Molecular-Orbital Studies of Organic-Molecules. *J. Chem. Phys.* **1972**, *56*, 2257−2261.

(33) Yanai, T.; Tew, D. P.; Handy, N. C. A New Hybrid Exchange-Correlation Functional Using the Coulomb-Attenuating Method (Cam-B3lyp). *Chem. Phys. Lett.* **2004**, *393*, 51−57.

(34) Cohen, A. J.; Mori-Sanchez, P.; Yang, W. Insights into Current Limitations of Density Functional Theory. *Science* **2008**, *321*, 792−794.

(35) Jensen, F. Describing Anions by Density Functional Theory: Fractional Electron Affinity. *J. Chem. Theory Comput.* **2010**, *6*, 2726−2735.

(36) Horke, D. A.; Li, Q.; Blancafort, L.; Verlet, J. R. R. Ultrafast above-Threshold Dynamics of the Radical Anion of a Prototypical Quinone Electron-Acceptor. *Nat. Chem.* **2013**, *5*, 711−717.

(37) Blokhin, A. P.; Gelin, M. F.; Khoroshilov, E. V.; Kryukov, I. V.; Sharkov, A. V. Dynamics of Optically Induced Anisotropy in an Ensemble of Asymmetric Top Molecules in the Gas Phase. *Opt. Spectrosc.* **2003**, *95*, 346−352.

(38) Horke, D. A.; Chatterley, A. S.; Verlet, J. R. R. Femtosecond Photoelectron Imaging of Aligned Polyanions: Probing Molecular Dynamics through the Electron-Anion Coulomb Repulsion. *J. Phys. Chem. Lett.* **2012**, *3*, 834−838.

(39) Verlet, J. R. R.; Horke, D. A.; Chatterley, A. S. Excited States of Multiply-Charged Anions Probed by Photoelectron Imaging: Riding the Repulsive Coulomb Barrier. *Phys. Chem. Chem. Phys.* **2014**, *16*, 15043−15052.

(40) Assion, A.; Geisler, M.; Helbing, J.; Seyfried, V.; Baumert, T. Femtosecond Pump-Probe Photoelectron Spectroscopy: Mapping of Vibrational Wave-Packet Motion. *Phys. Rev. A* **1996**, *54*, R4605−R4608.

(41) Kojima, H.; Urano, Y.; Kikuchi, K.; Higuchi, T.; Hirata, Y.; Nagano, T. Fluorescent Indicators for Imaging Nitric Oxide Production. *Angew. Chem., Int. Ed.* **1999**, *38*, 3209−3212.

(42) Miura, T.; Urano, Y.; Tanaka, K.; Nagano, T.; Ohkubo, K.; Fukuzumi, S. Rational Design Principle for Modulating Fluorescence Properties of Fluorescein-Based Probes by Photoinduced Electron Transfer. *J. Am. Chem. Soc.* **2003**, *125*, 8666−8671.

(43) Zhou, P. W.; Liu, J. Y.; Yang, S. Q.; Chen, J. S.; Han, K. L.; He, G. Z. The Invalidity of the Photo-Induced Electron Transfer Mechanism for Fluorescein Derivatives. *Phys. Chem. Chem. Phys.* **2012**, *14*, 15191−15198.

(44) Raffael, K.; Blanchet, V.; Chatel, B.; Turri, G.; Girard, B.; Garcia, I. A.; Wilkinson, I.; Whitaker, B. J. Time-Dependent Photoionization of Azulene: Optically Induced Anisotropy on the Femtosecond Scale. *Chem. Phys. Lett.* **2008**, *460*, 59−63.

(45) Schalk, O.; Hockett, P. Rotational Dephasing of Symmetric Top Molecules: Analytic Expressions and Applications. *Chem. Phys. Lett.* **2011**, *517*, 237−241.

(46) Chatterley, A. S.; West, C. W.; Roberts, G. M.; Stavros, V. G.; Verlet, J. R. R. Mapping the Ultrafast Dynamics of Adenine onto Its Nucleotide and Oligonucleotides by Time-Resolved Photoelectron Imaging. *J. Phys. Chem. Lett.* **2014**, *5*, 843−848.

(47) Chatterley, A. S.; West, C. W.; Stavros, V. G.; Verlet, J. R. R. Time-Resolved Photoelectron Imaging of the Isolated Deprotonated Nucleotides. *Chem. Sci.* **2014**, *5*, 3963−3975.

(48) Kanu, A. B.; Dwivedi, P.; Tam, M.; Matz, L.; Hill, H. H., Jr. Ion Mobility-Mass Spectrometry. *J. Mass Spectrom.* **2008**, *43*, 1−22.

(49) Uetrecht, C.; Rose, R. J.; van Duijn, E.; Lorenzen, K.; Heck, A. J. R. Ion Mobility Mass Spectrometry of Proteins and Protein Assemblies. *Chem. Soc. Rev.* **2010**, *39*, 1633−1655.

DOI: 10.1021/jz5022526
J. Phys. Chem. Lett. 2015, 6, 189−194